Direct Synthesis of Quantum Dots with Controllable Multimodal Size Distribution

Hsueh-Shih Chen* and Ramachandran Vasant Kumar

Department of Materials Science and Metallurgy, University of Cambridge, Pembroke Street, Cambridge CB2 3QZ

Received: March 20, 2009; Revised Manuscript Received: May 12, 2009

An approach to directly prepare quantum dots with a controllable multimodal size distribution in a simple one-pot synthesis is presented. In the case of bimodal size-distributed quantum dots, size group A is first grown in the initial stage, followed by a quenching process that can keep size group A in the chemical potential well (intermediate stable state) throughout the subsequent processes. Next, size group B is selectively grown by a series of injections of monomers in a low concentration conducted successively. Average sizes of size groups A and B can be individually controlled by the growth time in the initial stage and the temperature of successive injections of monomers in the last stage, respectively. This technique is also successfully extended to produce quantum dots with trimodal size distribution.

1. Introduction

Increasing energy problem relating to the perceived shortage of oil and concerns with growing carbon emissions has spurred scientists to develop new energy-saving techniques and materials. Colloidal semiconductor nanocrystals (NCs) or quantum dots (QDs), for example CdSe QDs, have received much attention to application of phosphors in white light emitting diodes (WLEDs), due to high photoluminescence (PL) efficiency, size-tunable emission wavelength, and photoexcitability by semiconductor chips.[1−6]

Precise control of particle size and size distribution is one of the key factors for applying QDs for practical applications. Under well-controlled experimental conditions, monodispersed (spherical), rod-like, or branched nanocrystals have been successfully synthesized by the so-called hot-injection approach.[4−6] In the case of monodispersed spherical CdSe QDs, injection of cold selenium precursor solution into hot cadmium/surfactant mixture leads to a burst of nucleation that consequently is suppressed by a sudden decrease of chemical potential due to consumption of monomers and/or with a lowering of growth temperature (20 °C lower than the injection temperature in general). These events diminish the nucleation rate and therefore separate the nucleation from the growth process. Decrease in monomer concentration in the vicinity of as-grown nuclei provides a diffusion-controlled growth regime in which the size-focusing event, that is, smaller QDs grow faster than bigger ones, benefiting reduction of size distribution can take place.[7,8] A typical size deviation of the QDs obtained is about 10 to 20% of nominated size in diameter or about 30 to 40 nm of the full width at half-maximum (fwhm) in PL spectra before any size separation technique is applied. Various sizes of the QDs from about 1 to 5 nm in diameter can be obtained by adjusting the growth time or the composition of the precursors.

In the general understanding of crystal growth, crystal nuclei compete with each other to grow into bigger crystals by consuming monomers from precursors and/or dissolution of particles smaller than the critical size in the growth process. So the size of as-grown particles should distribute within a range, as described by a continuous probability distribution or a monomodal size distribution, e.g., the normal (Gaussian) distribution. Control of monomodal size distribution for nanoparticles synthesized in liquid-phase has been developed in recent years.[9] In this work, we report a one-pot synthesis of colloidal QDs with controllable multimodal size distribution, which can simultaneously show multiple PL bands. The average size of the constituent size groups can be controlled by experimental factors based on the kinetics and thermodynamics. A possible mechanism is also presented to address the features of the experimental data. The suggested approach is not only potentially useful for future industrial applications, but is also valuable for providing further insight into the growth mechanism of QDs.

2. Experimental Section

2.1. Chemicals. All chemicals were used as received. Cadmium oxide (purity 99.99%), selenium (purity 99.999%), trioctylphosphine oxide (TOPO) (purity 90%), trioctylphosphine (TOP) (purity 90%), and 1-hexadecylamine (HDA) (purity 90%) were purchased from Aldrich. Stearic acid (SA) (purity 99%) and lauric acid (LA) (purity 99%) were purchased from Lancaster Synthesis. All solvents were purchased from Sigma-Aldrich (analytical grade).

2.2. Kinetic Perturbation Experiment. Cd precursor was prepared using 0.5 mmol of CdO, 2 mmol of SA or LA, 25 mmol of TOPO, and 40 mmol of HDA at 300 °C in a flask. TOPSe stock solution was prepared by dissolving 2 mmol of Se powder in 2.75 mmol of TOP and diluted by hexane to 7 mL. The QDs were first synthesized by an initial injection of 1-mL cold TOPSe into the hot Cd precursor at 280 °C. For the kinetic perturbation, six 1-mL TOPSe solutions were injected into the flask at 260 °C every minute from 180 s of growth time. An aliquot was taken from the system before each injection was performed for PL measurement.

2.3. Synthesis of QDs with Bimodal Size Distribution. TOPSe stock solution was first prepared by dissolving 2 mmol Se powders into 2.75 mmol TOP and diluted by hexane to 7 mL. Typically, the synthesis was divided into three stages. In stage I, i.e., preparation of QDs in size group A (A-QDs): 1 mL of TOPSe was injected in 3 s into a flask containing a CdO/SA/TOPO/HDA (0.5 /2 /25 /40 mmol) mixture at 280 °C and reacted to a desired particle size. In stage II, the system was

* To whom correspondence should be addressed. E-mail: hsc28@cam.ac.uk. Tel: +44 1223 334315. Fax: +44 1223 334567.

10.1021/jp9025317 CCC: $40.75
Published on Web 06/10/2009

immediately quenched below 220 °C (e.g., 170 °C) to suspend the A-QDs growth. In the stage III, i.e., synthesis of QDs in size group B (B-QDs), injections of monomers were successively conducted. Six 1-mL TOPSe solutions were injected into the system every minute. Each injection of TOPSe contained 0.286 mmol Se atoms.

For trimodal size-distributed QDs, growth processes of first two size groups (A-QDs and B-QDs) were similar to that of the bimodal size distributed QDs. In order to grow the third size group, the system is further quenched at lower temperature along with additional successive injections of monomers.

2.4. Measurement of Photoluminescence and Estimation of Particle Sizes. At the desired time, an aliquot was taken from the mixture for PL measurement. To reduce the disturbance from organic substances, all samples were washed by about 50× volume of methanol for three times before PL (Hitachi F-4500 Fluorescence Spectrophotometer) measurements.

Because the optical absorption bands of constituent size groups of QDs in multimodal size distribution overlapped each other, it was difficult to use UV−vis spectroscopy to estimate size and size distribution for QDs in the present study. Instead, PL spectra were used according to calibration data in the literature.[3,7,10] Despite the fact that the quantum yield of QDs may vary with particle size, it was expected that the quantum yield mainly slightly affects fwhm values and shows a minor effect on PL peak positions. For calculation of the standard deviation of QDs size, the quantum yields of all particles in the size groups are assumed to be the same. The mean sizes of QDs are directly translated from PL peak positions.

3. Results

3.1. Probabilistic Growth of QDs. In the thermodynamic regime, colloidal QD sizes would distribute in the normal distribution due to probabilistic and random collisions among particles and monomers. This phenomenon may be observed in PL spectra in form of the bell-shaped curve.[1−6] Previous studies have shown that kinetic factors such as an extra injection of monomers can be applied to boost the average growth rate and reduce the size distribution.[7] Accordingly, the kinetic regime is considered a way of QD synthesis to obtain QDs in an abnormal size distribution in the present study.

3.2. Kinetic Perturbation Experiment. First, a kinetic perturbation experiment is conducted to examine how extra monomers affect the size distribution of QDs. We performed a series of injections of a precursor (TOPSe) into a reaction system containing growing CdSe QDs and Cd monomers, and measured the PL spectra of an aliquot taken from the reaction mixture after each injection of the TOPSe was performed. As shown in Figure 1, before kinetic perturbation of extra monomers is carried out, a broad PL peak initially displays below 500 nm after 2 s of growth time (curve a), followed by a bell-shaped peak at 537 nm after 120 s (curve b), indicating that CdSe QDs has grown to a diameter of 2.58 nm ± 6.1% in the normal size distribution, where 6.1% is the standard deviation. The decrease in the PL fwhm of the CdSe QDs implies a size-focusing event as the growth rate of small nanocrystals is faster than that of large nanocrystals.[8,11] As the first extra TOPSe injection is introduced into the reaction system at 180 s, a shoulder appears by the major PL peak on the high energy side, as shown in Figure 1, curve c. This event manifests that the supplying of extra monomers can cause a variance for the normal distribution toward an unsymmetrical distribution. Further injections carried out successively every 60 s exhibit similar results as shown in Figure 1, curve d, which is measured after four extra injections

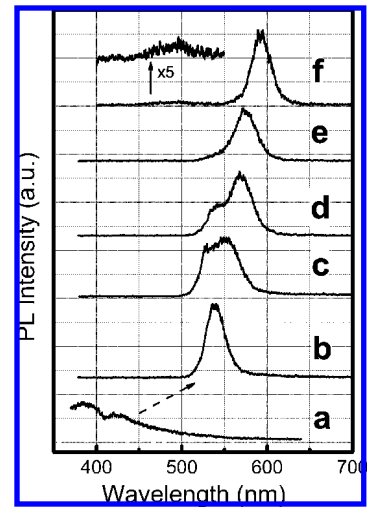

Figure 1. Typical PL spectra from CdSe QDs grown for 2 and 120 s (curves a and b) after an injection of TOPSe. The following extra injections of TOPSe are successively performed every 60 s, for example, the first injection is carried out at 180 s (curve c), the fourth injection is carried out at 360 s (curve d), and the sixth injection is carried out at 480 s (curve e). Curve f shows a PL spectrum of CdSe QDs grown by a slow injection of TOPSe at 280 °C (0.33 mL/sec).

are conducted. The size distribution recovers to normal after six injections are conducted, as shown in Figure 1, curve e. This kinetic perturbation experiment clearly highlights the fact that extra injections of monomers can alter the QDs size distribution during crystal growth.

3.3. Tail Band QDs. It is noticed that as-synthesized QDs usually reveal one main PL peak with a broadband tailing at the high energy side, even after the QDs purified by washing. The tail (TL) band implies the existence of smaller QDs nanocrystals in final products, probably resulting from variation in composition or temperature during QDs syntheses. For instance, if the nucleation and the growth are not well separated, e.g. slow injection rate or incidental fluctuation in temperature, a minority of small particles will accompany the majority, as shown in curve f in Figure 1. In general, the TL band may range 340−540 nm under 325-nm UV excitation and frequently peaks at around 390, 420, 470, 490, 506, and/or 525 nm depending on experimental conditions. Only under higher excitation energy (e.g., $\lambda_{ex} < 400$ nm) do the TL nanocrystals display emission, so they are often ignored or abandoned by size separation techniques.

In the present study, however, these TL nanocrystals will be used as seeds to grow QDs in other size groups. In brief, the growth of QDs in multiple size distribution is divided into three stages. In the stage I, QDs in the size group A (A-QDs) are first synthesized using a general approach in a reaction system as suggested in literatures.[5,6] In stage II, a quenching process is applied for the reaction system to suspend the A-QDs growth as a desired mean size of the A-QDs has been obtained. In stage III, a series of injections of precursors are successively injected into the reaction system to selectively grow TL seeds into QDs in the size group B (B-QDs, size B < A). In the present study, the A-QDs are reserved in the chemical potential well and kept in the original state during the growth process of the B-QDs (will discuss later).

4. Discussion

4.1. Growth of B-QDs. Figure 2 (curve a) plots a PL spectrum from A-QDs grown at 280 °C for 240 s. The bell-

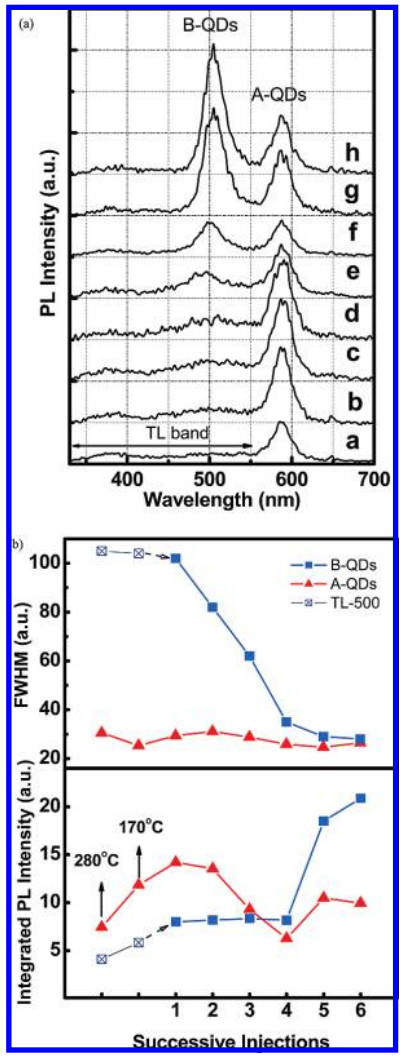

Figure 2. Temporal evolution of dual PL peaks from CdSe QDs in bimodal size distribution during successive injections of monomers. (a) Curve a shows a PL spectrum from A-QDs grown at 280 °C with an injection (reaction time = 4 min). Curve b shows a PL spectrum of the A-QDs collected at 170 °C. Curves c−h display PL spectra measured after 1−6 extra injections of monomers introduced at 170 °C. (b) The change in the fwhm and the integrated PL intensity for A-QDs and TL-500/B-QDs (curve TL-500).

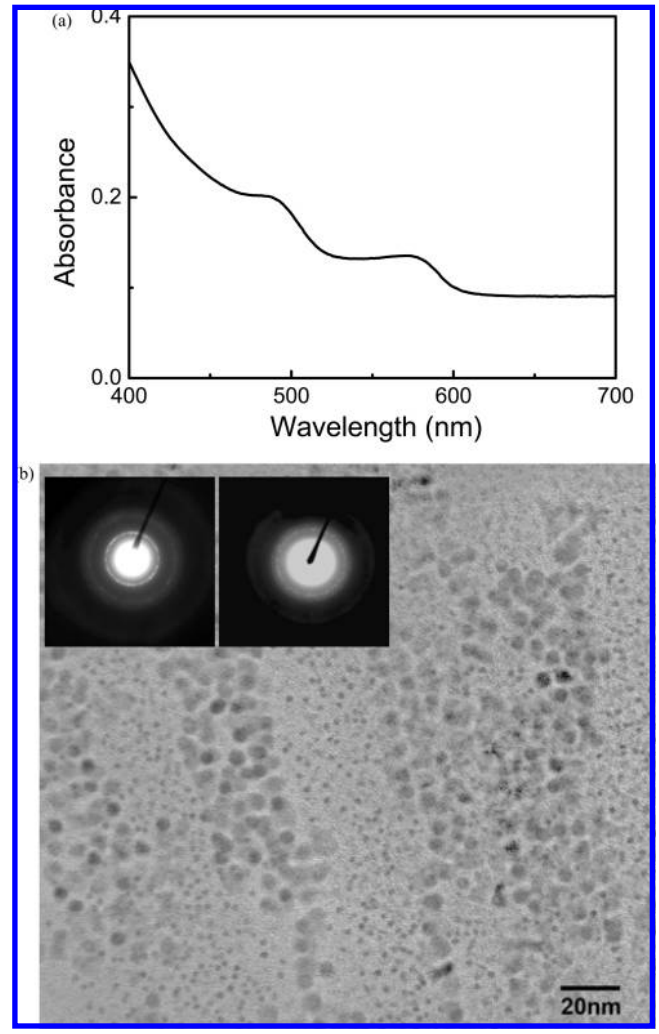

Figure 3. Optical absorption spectrum (a) and TEM images of CdSe QDs in bimodal size distribution (b). Insets in (b) are electron diffraction patterns of A-dots (left) and B-dots (right).

shaped PL peaks at 586 nm with fwhm about 29 nm corresponds to CdSe QDs in 3.6 nm ± 14% in diameter. As the reaction system is quenched to 170 °C (stage II), the PL peak shows no significant difference in position, suggesting that the A-QDs growth is effectively terminated, as shown in Figure 2 (curve b). Note that besides the A-QDs peak, a broad TL band is present between 340−550 nm. The TL band comprises two sub bands: one ranges from 340 to 450 nm (named as TL-380) and the other ranges from 450 to 550 nm (named as TL-500).

As extra injections of the TOPSe are conducted successively in the stage III, B-QDs are grown from the TL-500 seeds. As shown in Figure 2a (left peaks of curves e−h), the TL-500 band gradually heightens with an increase in the number of the monomers injections. Integrated intensity of the TL-500 band rises slightly in the first four injections, but suddenly soars after the fifth injection is carried out, as shown in Figure 2b. This phenomenon implies that the extra monomers make the concentration exceed a critical point and trigger the regrowth for the TL-500 QDs. A separate PL peak finally peaks at 506 nm, indicating that B-QDs in a distinct size group are developed. The fwhm of the second PL peak largely decreases from 102 to 35 nm, representing that the size distribution significantly reduces from the TL-500 seeds to the B-QDs.

Final QD products display dual PL peaks at 506 nm (fwhm = 28.1 nm) and 586 nm (fwhm = 26.4 nm), which corresponds to two distinct size groups: 2.2 nm ± 9% and 3.6 nm ± 9% Figure 3a shows an optical absorption spectrum of the CdSe QDs being in the bimodal size distribution. The spectrum appears to involve two excitonic absorption peaks at around 574 and 492 nm from the A-QDs and the B-QDs in the QDs ensemble. Figure 3b shows transmission electron microscope (TEM) images of the QDs. Note that organic remains from precursors and defocus of images due to difference of the focus planes between the A-QDs and the B-QDs may affect the image quality. Electron diffraction patterns show that both A-QDs and B-QDs are crystalline, as shown in Figure 3b (insets).

4.2. Thermodynamics and Chemical Potential Well. In general, concentration or temperature variation can cause growth or dissociation of crystals in growth according to the Gibbs−Thomson relationship. Thus, both of particles size and size distribution will change if monomers concentration increases. This fact has been confirmed by the kinetic perturbation experiment, as shown in Figure 1. However, the situation may be different if particles are in a certain stable state, for example,

SCHEME 1: Chemical Potential Well from the Magic Closed-Shell Structure for QDs[a]

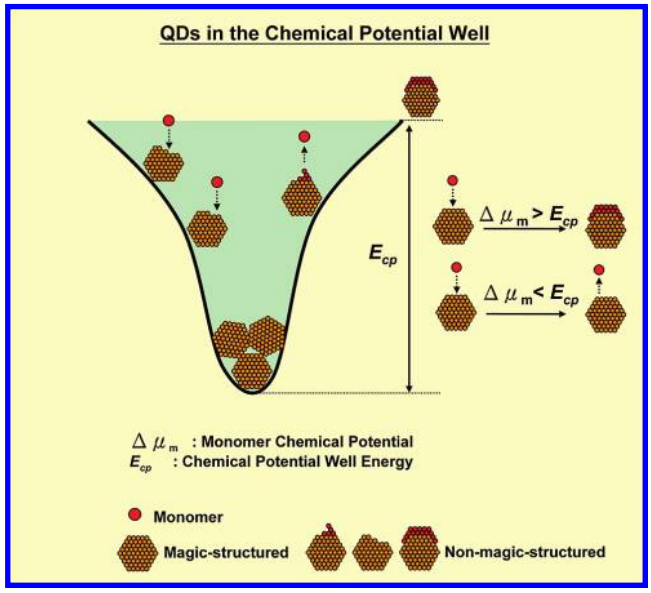

[a] The monomer chemical potential is relative to the surface of QDs.

particles in the magic size. The magic-sized particles would stay in the original state to some extent due to a relatively high stability.

It has been known that CdSe molecular clusters composed of 13, 17, 26, 35, 48, 69, and 72 CdSe pairs show the local minimum of total energy of CdSe pair and the maximum relatively stability.[12] These magic numbers are unique and correlate to specific sizes. This result has been extended to explain that CdSe nanocrystals in the magic closed-shell structure, corresponding to 2.2 or 3.4 nm in diameter, are thermodynamically stable and have relative maximum PL efficiency as the closed-shell QDs surface is stacked by the most coordinated atoms.[13] Consequently, these magic-sized molecular clusters or nanocrystals are thought to be in a relative low energy state, namely in an energy well in the classic size-chemical potential curve from thermodynamics. This chemical potential well plays an important role in crystal growth. In our preliminary study, we found that growth rate of CdSe QDs dramatically reduces in the range from 3.4 to 3.7 nm due to high stability of the CdSe QDs in the chemical potential well.[14] Scheme 1 illustrates the chemical potential well for QDs in the closed-shell morphology. The chemical potential well preserves the closed-shell QDs to some extent from external disturbances of energy. The growth of the closed-shell QDs would only take place when the monomer chemical potential $\Delta\mu_m$ relative to QDs surface is larger than the potential well energy E_{cp}. However, If $\Delta\mu_m < E_{cp}$, the crystal growth could not proceed until sufficient chemical potential is provided. This phenomenon signifies that QDs are able to be fixed in some specific sizes having lower energy states during the growth process if sufficient chemical energy is removed from a reaction system and the subsequent fluctuation of the chemical energy is smaller than the E_{cp}.

The A-QDs keep their original state throughout the B-QDs growth process. As shown Figure 2 (right peaks of curves c−h), there is no change in the PL peak position of the A-QDs during both the quenching and the growth processes of the B-QDs, revealing that the A-QDs are constrained in the chemical potential well. The stage of decreasing temperature to 170 °C is essential. In a higher temperature, e.g., 280 °C, A-QDs will grow up to ~4 nm under the same experimental conditions due to that the $\Delta\mu_m$ can be high enough to drive the A-QDs to overcome the potential well energy ($\Delta\mu_{m\text{-}280\ ^\circ C} > E_{cp,\ A\text{-}QDs}$). So some thermal energy must be removed from the reaction system to suspend the A-QDs growth (e.g., quench to 170 °C), making $\Delta\mu_{m\text{-}170\ ^\circ C} < E_{cp,\ A\text{-}QDs}$ that places the A-QDs in the potential well, as shown in curve a and b. The μ_{si} generated by subsequent injections of monomers to grow B-QDs obviously does not make the ($\mu_{si} + \Delta\mu_{m\text{-}170\ ^\circ C}$) exceed the $E_{cp,\ A\text{-}QDs}$ as the A-QDs keep their size during the process.

In contrast to A-QDs, the TL seeds can develop to B-QDs by extra injections of monomers as the smaller TL seeds have a higher reactivity. The TL seeds should be in the form of certain stable configurations as they are found in final products. In fact, the TL seeds are somewhat like the closed-shell A-QDs having a relatively stable state. It has been found that magic-sized CdSe clusters exhibit sharp optical absorption in the range from 350 to 450 nm, for example, 350−360, 384, 406, and 431−447 nm.[15,16] These optical absorption data correspond to about 380−470 nm in PL spectra. Hence, it may be considered that the TL seeds comprise those stable molecular clusters and nanocrystals. It should be emphasized that those smaller nanocrystals may emit some PL signals due to the recombination of carriers from the surface state. In addition, Peng et al. has proposed that magic-sized CdSe molecular clusters have a relatively low energy state that does not obey the Gibbs−Thompson relationship,[5] which is similar to QDs in the closed-shell morphology in the present study. Thus, the chemical potential well would be present in the growth process for both molecular clusters and nanocrystals.

The existence of the chemic potential well for the TL seeds could be demonstrated by the change in PL intensity integrated between 450 and 550 nm. As shown in the TL-500 curve in Figure 2b, the integrated PL intensity shows only slight increase in the first four injections, indicating the extra monomers do not significantly influence TL seeds/B-QDs that in the stable state. After the fifth injection of monomers is conducted, the integrated PL intensity apparently increases and peak position shifts to 506 nm. This event implies that accumulated supersaturation of monomers finally exceed the potential barrier, i.e. $\mu_{si} + \Delta\mu_{m\text{-}170\ ^\circ C} > E_{cp,\ TL\text{-}seeds}$. So the TL seeds can regrow into next stable configuration (i.e., B-QDs) and stop growing when $\mu_{si} + \Delta\mu_{m\text{-}170\ ^\circ C}$ is smaller than $E_{cp,\ B\text{-}QDs}$. The B-QDs are 2.2 nm that is also close to a reported closed-shell size.[12,13] Moreover, the PL fwhm rapidly reduces during the extra injections of the monomers. This is due to the sharpening of the B-QD's PL peak. So the B-QDs may be considered the size narrowing of the TL-500 seeds.

4.3. Growth Mechanism of Multimodal Size Distribution. Despite the fact that the extra monomers do not provide sufficient energy for the A-QDs growth, they do result in oscillations in fwhm values and PL integration intensity (from 550 to 650 nm), as shown in Figure 2b. The oscillation in PL intensity is thought to be the adjustment of morphology/size to the relative stable state during the successive injections of extra monomers and/or temperature fluctuations for the A-QDs. The reaction of the process can be expressed as the following set of equations.

$$[\mathrm{Cd}] + [\mathrm{Se}] \xrightarrow{280^\circ C} (\text{A-QDs}) + (\text{TL-Seeds}) + [\mathrm{Cd}]' + [\mathrm{Se}]' \quad (1)$$

$$[\mathrm{Cd}]_{170^\circ\mathrm{C}} + [\mathrm{Se}]_{170^\circ\mathrm{C}} \xleftrightarrow{170^\circ\mathrm{C}} (\text{A-QDs})_{\mathrm{cp}} + (\text{TL-Seeds})_{\mathrm{cp}} + [\mathrm{Cd}]'_{170^\circ\mathrm{C}} + [\mathrm{Se}]'_{170^\circ\mathrm{C}} \quad (2)$$

$$[\mathrm{Cd}]'_{170^\circ\mathrm{C}} + [\mathrm{Se}]'_{170^\circ\mathrm{C}} + (\text{A-QDs})_{\mathrm{cp}} + (\text{TL-Seeds})_{\mathrm{cp}} + [\mathrm{Se}]_{\mathrm{si}} \xrightarrow{170^\circ\mathrm{C}} (\text{A-QDs})_{\mathrm{cp}} + \langle(\text{TL-Seeds})_{\mathrm{cp}} + [\mathrm{Se}]'' + [\mathrm{Cd}]''\rangle + [\mathrm{Cd}]''_{170^\circ\mathrm{C}} + [\mathrm{Se}]''_{170^\circ\mathrm{C}} \quad (3)$$

$$[\mathrm{Cd}]_{\mathrm{eqm}} + [\mathrm{Se}]_{\mathrm{eqm}} \xleftrightarrow{170^\circ\mathrm{C}} (\text{A-QDs})_{\mathrm{eqm}} + (\text{B-QDs})_{\mathrm{eqm}} + [\mathrm{Cd}]''_{\mathrm{eqm}} + [\mathrm{Se}]''_{\mathrm{eqm}} \quad (4)$$

where the subscript cp indicates QDs in the chemical potential well. At 280 °C, an initial injection of cold TOPSe into hot Cd precursor produces extremely high concentration of monomers [Cd] and [Se], and results in a rapid formation of A-QDs and TL seeds. [Cd]′ and [Se]′ refer to unreacted monomers (eq 1). When the system is quenched below 220 °C, for example 170 °C, A-QDs and TL seeds can be preserved in the chemical potential well as shown in eq 2. If a certain amount of TOPSe is injected into the system to produce extra monomers $[\mathrm{Se}]_{\mathrm{si}}$, then the reaction will proceed toward the right. The overall chemical potential of monomers has no sufficient driving force for the regrowth of A-QDs in the chemical potential well with barrier $E_{\mathrm{cp,\ A\text{-}QDs}}$, but it is able to cause regrowth of the TL seeds (eq 3) toward B-QDs. Finally, QDs product obtained will be in bimodal size distribution as the reaction reaches equilibrium (eq 4). The growth mechanism along with the chemical potential-size curve involving a series of the chemical potential wells are schematically shown in Scheme 2. The strategy to grow multimodal size distributed QDs is that the overall chemical potential of monomers ($\mu_{\mathrm{si}} + \Delta\mu_{\mathrm{m}}$) must not exceed the chemical potential well barriers of A-QDs or B-QDs, but the ($\mu_{\mathrm{si}} + \Delta\mu_{\mathrm{m}}$) is sufficient to trigger the regrowth of TL seeds.

4.4. Control of Mean Size for Constituent Size Groups. Mean sizes of A-QDs and B-QDs can be individually controlled by growth time in stage I and temperature of extra injections of monomers in stage III, respectively. In Figure 4a, PL peak position of A-QDs red shifts from about 550 to 600 nm with increase of growth time, while B-QDs are kept at around 520 nm in all exercises. This result demonstrates that A-QD's mean size can be individually between 2.8−4.0 nm without any influence on B-QDs mean size. However, B-QDs' mean size can also be individually adjusted from about 460−540 nm, corresponding to 1.6−2.6 nm in diameter, by temperature of the successive injections of monomers, as shown in Figure 4b. With an increase in temperature of the successive injections from 130 to 200 °C, the B-QDs' PL wavelength increases. However, B-QDs could not appear below 130 °C or above 200 °C. The events are understandable; if the temperature is below 130 °C, then the monomer's chemical potential is so low that the TL seeds could not grow even if extra monomers are introduced into the system. However, if the temperature is above 200 °C, then B-QDs will directly pass over the potential barrier and grow into bigger particles. This case is similar to the data

SCHEME 2: Illustration of the Reaction Process and the Mechanism of the QDs with Multimodal Size Distribution[a]

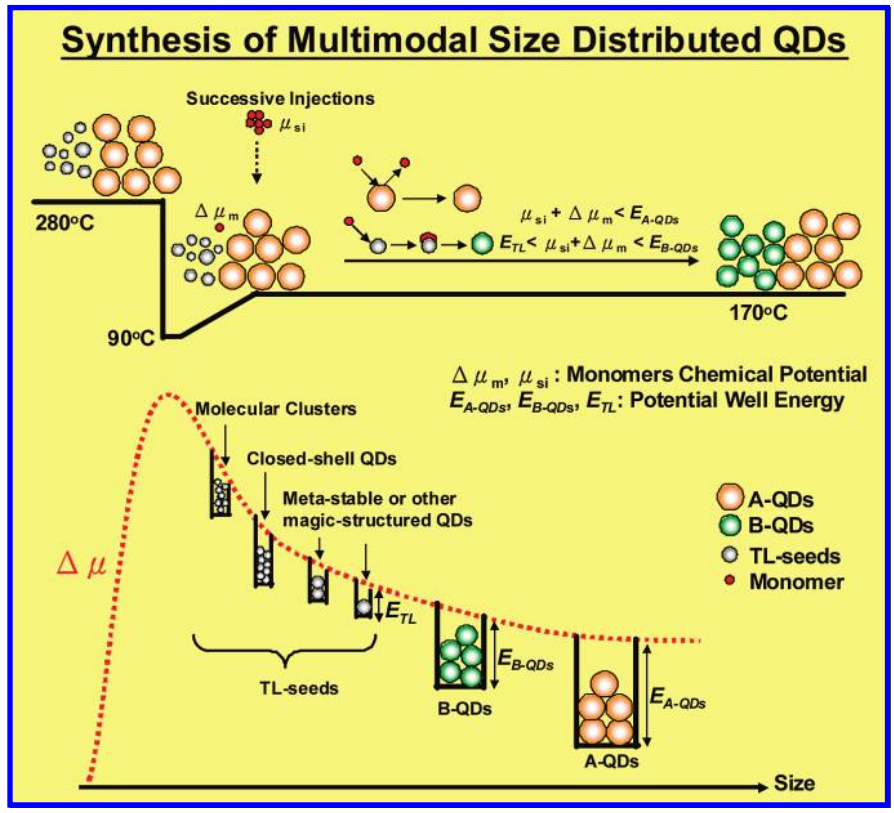

[a] The $\Delta\mu_{\mathrm{m}}$ and μ_{si} are the chemical potential for unreacted monomers and extra monomers from successive injections, respectively.

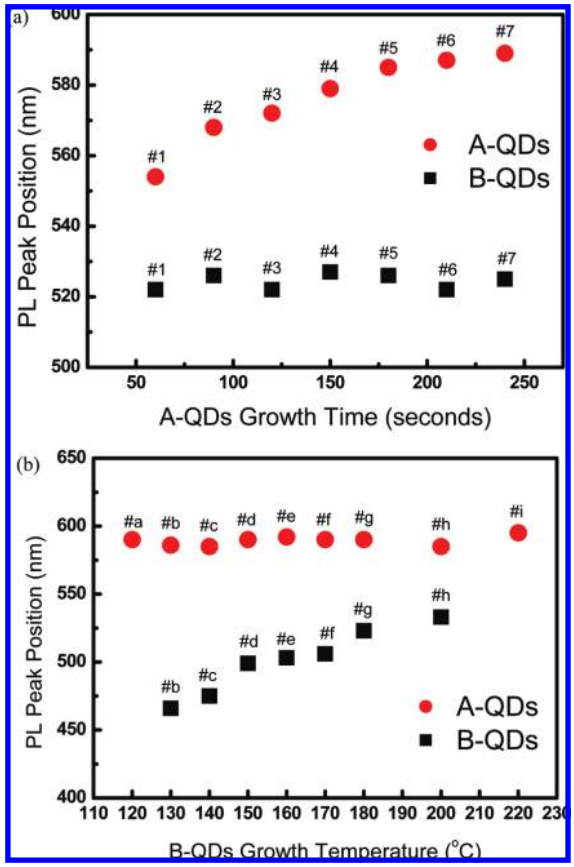

Figure 4. Control of PL wavelength for A-QDs and B-QDs in an ensemble. (a) In exercises #1−#7 (synthetic parameters of B-QDs are fixed), A-QDs are grown at 280 °C for 60 (#1), 90 (#2), 120 (#3), 150 (#4), 180 (#5), 210 (#6), and 240 (#7) s in stage I. B-QDs are grown at 170 °C in the stage II in all exercises. (b) In exercises #a−#i (synthetic parameters of A-QDs are fixed), A-QDs are first grown at 280 °C for 240 s. B-QDs are prepared by six injections of monomers performed at 120 °C (#a), 130 °C (#b), 140 °C (#c), 150 °C (#d), 160 °C (#e), 170 °C (#f), 180 °C (#g), 200 °C (#h), and 220 °C (#i). Note that samples only show A-QDs PL peak at 120 and 220 °C.

in Figure 1, where the injected monomers contribute to both size and size distribution for the A-QDs. In fact, this phenomenon resembles the size-focusing event.[7] Accordingly, the size-focusing event may be considered a special case in the present study. In addition, nanocrystals with bimodal size distribution were also observed in dissolution/ripening experiments of nanocrystals at elevated temperature s (e.g., 300 °C), and were connected to an interparticle interaction.[17]

For the preservation of A-QDs in the chemical potential well, the removal of thermal energy is a key step. Injections of extra monomers in regular succession play an essential role in the kinetic generation of B-QDs. Each of the injections contains limited monomers, preventing a rapid increase in supersaturation that may cause the regrowth of A-QDs. A continuous feeding system of monomers may produce a similar result. Remarkably, the initial concentration of Cd monomers is seen to affect the formation of B-QDs. For instance, B-QDs cannot form if the initial Cd monomer concentration is very low. This may be due to exhaustion of Cd monomers consumed by A-QDs in the stage I. Details will be published elsewhere.

On the basis of the strategy of synthesis of bimodal size distributed QDs, trimodal size-distributed QDs have been obtained as well, as shown in Figure 5. The fist PL peak at 615 nm (fwhm ≈ 27 nm) is first prepared at 280 °C for 25 min of

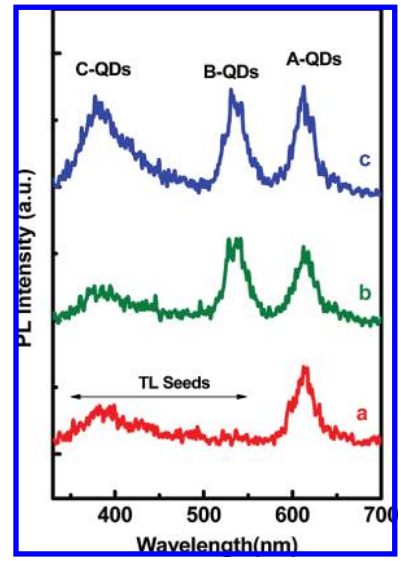

Figure 5. CdSe QDs in trimodal size distribution synthesized in a one-spot synthesis. The A-QDs at 615 nm are first prepared at 280 °C for 25 min of growth time (curve a). Then the B-QDs at 535 nm and C-QDs at 380 nm are prepared by three successive injections of monomers for each at 200 and 140 °C, respectively (curves b and c).

the growth time. The second PL peak at 535 nm (fwhm ≈ 28 nm) is then obtained at 200 °C via three successive injections of TOPSe. The last peak at 380 nm (fwhm ≈ 60 nm) is synthesized at 140 °C by another three injections in succession. The final QD product is in trimodal size distribution: 4.6 nm ± 12%, 2.5 nm ± 6%, and 0.8 nm ± 32%.

5. Conclusions

QDs with controllable bimodal size distribution have been successfully synthesized. The strategy is to prepare QDs in size group A in the first stage, followed by a quenching process that can keep the QDs in the original state in subsequent processes. QDs in size group B are generated from TL seeds by extra injections of monomers conducted successively every minute. The mean sizes of constituent size groups A and B could be individually controlled by the growth time in the first stage and the temperature of successive injections of monomers in the last stage, respectively. This technique is successfully extended to produce QDs with trimodal size distribution. We have proposed a model based on the chemical potential well from stable morphologies of QDs, such as the closed-shell structure to address the experimental features. These results are expected to lead to further development in the growth kinetics and control of size distribution for nanocrystals.

References and Notes

(1) Chen, H. S.; Wang, S. J. J.; Lo, C. J.; Chi, J. Y. *Appl. Phys. Lett.* **2005**, *86*, 131905.
(2) Bowers II, M. J.; McBride, J. R.; Rosenthal, S. J. *J. Am. Chem. Soc.* **2005**, *127*, 15378–15379.
(3) Chen, H. S.; Hsu, C. K.; Hong, H. Y. *IEEE Photon. Tech. Lett.* **2006**, *18*, 193–195.
(4) Manna, L.; Scher, E. C.; Alivisatos, A. P. *J. Am. Chem. Soc.* **2000**, *122*, 12700–12706.
(5) Peng, Z. A.; Peng, X. *J. Am. Chem. Soc.* **2002**, *124*, 3343–3353.
(6) Chen, H. S.; Lo, B.; Hwang, J. Y.; Chang, G. Y.; Chen, C. M.; Tasi, S. J.; Wang, S. J. *J. Phys. Chem. B* **2004**, *108*, 17119–17123.
(7) Peng, X.; Wickham, J.; Alivisatos, A. P. *J. Am. Chem. Soc.* **1998**, *120*, 5343–5344.
(8) Qu, L.; Yu, W. W.; Peng, X. *Nano Lett.* **2004**, *4*, 465–469.

(9) Mantzaris, N. V. *Chem. Eng. Sci.* **2005**, *60*, 4749–4770.
(10) Jun, S.; Jang, E. *Chem. Commun.* **2005**, 4616–4618.
(11) Peng, X.; Manna, L.; Yang, W.; Wickham, J.; Scher, E.; Kadavanich, A.; Alivisatos, A. P. *Nature* **2000**, *404*, 59–61.
(12) Yu, M.; Fernando, G. W.; Li, R.; Papadimitrakopoulos, F.; Shi, N.; Ramprasad, R. *Appl. Phys. Lett.* **2007**, *88*, 231910.
(13) Yu, M.; Fernando, G. W.; Li, R.; Papadimitrakopoulos, F.; Shi, N.; Ramprasad, R. *J. Comput.-Aided Mater. Des.* **2007**, *14*, 167–174.
(14) Chen, H. S.; Kumar, R. V. *J. Phys. Chem. C* **2009**, *113*, 31–36.
(15) Kudera, S.; Zanella, M.; Giannini, C.; Rizzo, A.; Li, Y.; Gigli, G.; Cingolani, R.; Ciccarella, G.; Spahl, W.; Parak, W. J.; Manna, L. *Adv. Mater.* **2007**, *19*, 548–552.
(16) Wang, H.; Tashiro, A.; Nakamura, H.; Uehara, M.; Miyazaki, M.; Watari, T.; Maeda, H. *J. Mater. Res.* **2004**, *19*, 3157–3161.
(17) Thessing, J.; Qian, J.; Chen, H.; Pradhan, N.; Peng, X. *J. Am. Chem. Soc.* **2007**, *129*, 2736–2737.

JP9025317